CHEMICAL TREATMENT AND MODIFICATION OF JUTE FIBER SURFACE

Bruno de Paula Amantes[1], Renato Pereira de Melo[1], Roberto Pinto Cucinelli Neto[1],
*Maria de Fatima Vieira Marques[1], ***

Abstract. In this work, jute fiber was used as a source of cellulose fiber. Chemical processes for the purification, mechanical dispersion in Ultra Turrax and modifications with titanium isopropoxide (TiP), 3-aminopropyl-trimethoxysilane (APTMS), as well as double modification with both TiP and APTMS, were used to obtain fibers with reduced diameter and less agglomeration and adhesion to polar polymers such as polyamides. Fibers with a diameter close to 10 μm were observed by SEM after drying and pulverization. The fibers subjected to alkaline treatment, acid hydrolysis and doubly modified were well dispersed in water. SEM micrographs revealed the obtainment of fibers with a diameter close to 1 μm for those modified with TiP and APTMS. NMR results exhibited a reduction in the amplitude index accompanied by an increase in the relaxation time and in thickness of the crystalline domains by the removal of lignin and hemicellulose. A contrary effect was observed with the chemical modifications. The results of FTIR and XDR also indicated the removal of lignin and hemicellulose, as did the chemical modifications of cellulose. Increased crystallinity index (CI) was observed with the removal of amorphous components in jute fiber, while CI declined in the fiber modified with both TiP and APTMS. However, TGA results showed higher resistance to thermal degradation for the doubly modified fiber.

Keywords: jute fiber, cellulose, titanium oxide, silanization.

1. Introduction

Cellulose is a naturally occurring semicrystalline polymer obtained from numerous sources, but it is mainly present in wood biomass. Cellulose fiber among others can be applied in automobiles, building materials, packaging, and pharmaceuticals, as well as in biomedicine. The extensive use of cellulose is due to its low environmental impact and other specific characteristics, such as renewability, biodegradability, low density, good mechanical properties, non-abrasive nature, and easy surface modification. On the other hand, its low thermal resistance and high hydrophilicity limit its application.

Numerous chemical and mechanical treatments have been attempted to purify and modify the surface as well as isolate cellulose nanofibers (CNFs) [1, 2] or cellulose nanocrystals (CNWs). Structurally, natural fiber is organized into fibrils that are covered by a matrix of lignin and hemicellulose [3-5]. Eliminating these amorphous components from cellulose will increase thermal resistance and degree of crystallinity of the fibers. CNFs are composed of purified cellulose fibrils that contain both amorphous and crystalline domains. The amorphous regions of the cellulose structure act as structural defects in fibrils and are responsible for the transverse cleavage of microfibrils during hydrolysis with strong acids at high concentrations, isolating needle-like crystal structures called cellulose nanocrystals or nanowhiskers (CNWs), which are highly crystalline. CNWs have strong mechanical properties (Young's modulus and tensile strength) but considerably lower aspect ratio and degradation temperature compared to CNFs [5-8], which decreases the reinforcing effect on polymers, preventing the preparation of polymer composites that require high processing temperatures.

Cellulose nanofibers (CNFs) contain fibrils with length of several micrometers and diameter in the nanometric range (size 1–100 nm), forming a network structure. CNFs can be prepared by the release of the constituent fiber matrix and microfiber bundles [9, 10]. As previously mentioned, nanofibrils contain amorphous and crystalline cellulosic regions and are generally produced by delamination of wood pulp through mechanical pressure before and/or after chemical or enzymatic treatment [11-16]. Chen *et al.* [2] identified nanocellulose fibers from wood pulp using chemical pretreatment and

[1] Universidade Federal do Rio de Janeiro,
Instituto de Macromoléculas Eloisa Mano, IMA-UFRJ,
Cidade Universitária. Av. Horácio Macedo, 2.030.
Centro de Tecnologia. Bloco J. Rio de Janeiro. RJ. Brasil.
* *fmarques@ima.ufrj.br*

high intensity ultrasound. In another work [1], the authors used bamboo fibers to obtain ultra-long CNFs with crystal form of cellulose I of lengths greater than 1 mm and 30–80 nm in diameter, by applying conventional chemical pretreatment combined with high-intensity ultrasonication followed by freeze drying. CNFs were prepared from banana and pineapple fibers employing the steam blast technique under different conditions, followed by mechanical stirring [17, 18]. Other chemical and mechanical processes for nanocellulose isolation are found in the literature [12]. However, one of the drawbacks of chemical purification of natural fibers is hornification [19] – a process where cellulose fibers properties are changed due to repeated morphological and chemical alterations during drying. Additional hydrogen bonds between the amorphous portions of the fibrils formed during drying are considered irreversible even under conditions that normally lead to bond breakage. This irreversibility is decreased according to the amount of the lateral bond between fibers. This is due to the reduced accessibility of the hydroxyl groups [20, 21]. To prevent hornification during cellulose refining, purification is preferably done with the pulp in an aqueous suspension, since it is not possible to dry nanofibers without the occurrence of irreversible agglomeration.

Agglomeration between CNFs occurs due to strong hydrogen bonding interactions, reducing their aspect ratio and their reinforcement potential when inserted into a polymer matrix. These interactions can be reduced by the introduction of steric and electrostatic groups [20] on the fiber surface. During acid hydrolysis *via* sulfuric acid, sulfate groups are formed on the surface of the microfibrils, creating a double layer with electrical repulsion between the suspended fibrils, helping in their dispersion [22].

Titanium oxide has been of interest because it is a nontoxic and biocompatible material and possesses antibacterial activity, acting as a photocatalyst of organic material degradation. TiO_2 coating of natural fibers is a process with potential in the textile industry for its properties, including self-cleaning by the decomposition of organic dirt, environmental pollutants and harmful microorganisms, but it requires UV radiation for antibacterial application [23-26]. The deposition of TiO_2 on the surface of cellulose fiber can be performed from the controlled hydrolysis of titanium oxysulfate in the presence of cellulose fiber [27]. Moreover, the condensation of titanium isopropoxide (TiP) on the surface of the cellulose fiber using the sol-gel method was previously described [28, 29]. On the other hand, silanes are recognized as efficient coupling agents and are extensively used in the formulation of polymers and adhesives. They have been successfully applied in inorganic fillers such as glass fiber and silica to reinforce polymer composites. The bifunctional structures of silanes have also been of interest for application in natural fiber/polymer composites, since both glass fiber and natural fiber have reactive hydroxyl groups [30, 31].

The present study is aimed to obtain purified and modified cellulose fibrils from natural jute fibers with low diameter caused by chemical modification of their surfaces after acid hydrolysis at low concentration and to forming TiO_2 by impregnation of TiP in the hydroxyl groups of cellulose. Further chemical modification with APTMS was performed to increase the chemical affinity between the fibers and polar polymers such as polyamides. Fibers obtained during all the refining treatment steps as well as the modified fibers were analyzed by low-field nuclear magnetic resonance (NMR), scanning electron microscopy (SEM), Fourier-transform infrared spectroscopy (FTIR), X-ray diffractometry (XRD), and thermogravimetric analysis (TG).

2. Experimental

2.1. Materials

Jute fiber received from Pematec Triangel Brazil was used as a source of cellulose fibers. Sodium chlorite P.A. (Sigma-Aldrich), glacial acetic acid (TEDIA High Purity Solvents), sodium hydroxide P.A., sulfuric acid P.A., anhydrous methanol, 99.8% (Sigma-Aldrich), isobutanol (Vetec Química Fina Ltda), (3-aminopropyl) trimethoxysilane 97% (APTMS), and titanium(IV) isopropoxide (TiP) 97% (Sigma Aldrich) were used without further purification.

2.2. Chemical Purification of Cellulose from Jute Fibers

The purification of raw jute fibers was performed according to the literature [1, 2] with some modifications. Before chemical treatments, the fibers were cut with scissors and then milled in a knife mill (SOLAB SL-32) with screen of 10 mesh (sample JF). In the first purification step, most of lignin was removed. A suspension of 20 g of fiber and 600 ml of acidified sodium chlorite (3 wt %) solution containing acetic acid (pH=4) was prepared in a glass flask and heated at 348 K for an hour with mechanical stirring. This extraction was repeated three times, resulting in sample JF_Cl. In the next step, the JF_Cl fiber was treated with 6 wt % sodium hydroxide solution at 353 K for 1 h and mechanical stirring to remove most hemicellulose. This process was also repeated three times, resulting in alkalized jute fiber (JF_al). The JF_al fiber was suspended in distilled water, placed under mechanical stirring in an ice bath while

concentrated sulfuric acid was added dropwise until the desired acid concentration was reached (10 wt %). This suspension was heated under stirring to 313 K and maintained for 4 h and the last treatment step was performed with a 2 wt % sodium hydroxide solution at 353 K for 1 h, obtaining the hydrolyzed fiber JF_ha. To facilitate purifying of the jute fibers, they were soaked in water until complete purification. The JF_ha fiber was dried overnight at 333 K. Then, 5 g of fiber was pulverized in an A11 Basic Analytical mill (IKA) with stainless steel blade.

2.3. Treatment with Titanium Isopropoxide

The pulverized fibers were dispersed in 250 ml of isobutanol by a T25 digital Ultra-Turrax for 2 min at 20,000 rpm. A solution was prepared with 0.53 g of TiP in 5 ml of isobutanol. In a glass flask under mechanical stirring, the TiP solution was added dropwise to the fiber suspension under vigorous stirring at room temperature for 10 min. Then, reaction was carried out for one hour at room temperature at reduced stirring speed and then for additional 20 min at 333 K. The fibers were filtered and washed with distilled water and dried overnight under vacuum at 333 K, obtaining the titanium modified fiber (JF_Ti) [28, 32].

2.4. Treatment with APTMS

The silanized fiber (JF_APTMS) was obtained in a similar way; but the solutions were prepared with methanol. The silane solution was prepared with 0.12 g of APTMS in 5 ml of methanol. In a glass flask under mechanical stirring, the APTMS solution was added dropwise to the fiber suspension. The pH was maintained in a range between 4.5 and 5.5. The reaction occurred for one hour at room temperature and then for additional 20 min at 333 K [33]. The fibers were filtered, washed with distilled water and dried overnight under vacuum at 333 K.

2.5. Treatment with Both Titanium and Silane Compounds

Table 1

Codes of the samples and their treatments

Sample Code	Fiber treatment
JF	Raw jute fiber
JF_Cl	With sodium chlorite
JF_al	With alkali
JF_ha	Hydrolyzed with 10 wt % H_2SO_4
JF_Ti	Titanized jute fiber
JF_APTMS	Silanized jute fiber
JF_Ti+APTMS	With both Ti and silane

The third material was prepared as described before. The JF_ha was surface modified with TiP and then with APTMS, obtaining a doubly modified fiber (JF_Ti+APTMS).

Table 1 summarizes the description of the treatments performed on jute fibers.
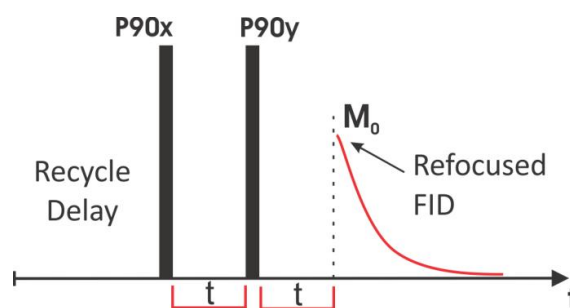
2.6. Characterization

Visual Test

The jute fiber purification was also accompanied visually by the change in the raw fiber suspensions and fibers obtained at each stage of chemical treatment. The fibers were mechanically dispersed by Ultra-Turrax in water, methanol and isobutanol at the ratio 1/50 (fiber/medium). Portions of the suspensions were immediately transferred to glass flasks and were observed after 30 min. rest.

Low-field NMR measurements

Analyses were performed in a Maran Ultra 0.54 T low-field NMR (23.4 MHz for ^{1}H), operating at 303 K. For all samples, a known mass was placed in a tube with 18 mm diameter and left at rest for 10 min in the equipment for thermal stabilization.

Solid echo pulse and inversion-recovery pulse sequences were used. The first one was conducted to measure the amplitude indices of each sample. The second was to evaluate the effect of fiber structural changes on the morphology of the chains, specifically in domains with a thickness of 15–20 nm.

Solid echo is a sequence of pulses designed to refine systems of up to two spins that have strong dipole coupling, making up the entire decay signal, without dead time interference. Basically, it consists of a hard 90° pulse followed by another 90° pulse and a hard -90° with the use of suitable phase cycling. In this work, the time between pulses (*t*) was 3 μs, the 90° pulse used was 7.5 μs and the decay signal was composed of 2048 points for 1 μs (Fig. 1). Sixty-six replicates were performed with a 2-second waiting time between them.

Fig. 1. Sequence of solid echo pulses. The indices x and y refer to the phase cycling, where x = 0213 and y = 1122

The initial and maximum signal of the decay (M_0) obtained is directly proportional to the molar fraction of hydrogen present in the sample. Eq. (1) shows that the ratio between M_0 and sample mass (m) is the amplitude index (AI, eV/g), which can be used in numerous studies to monitor the variation of the amount of hydrogen as a function of chemical reactions.

$$AI = \frac{M_0}{m} \qquad (1)$$

The inversion-recovery pulse sequence ($p180x$-t-$p90x$) was used to obtain the longitudinal relaxation time (T_1H) of the samples and for evaluation of domains on a 15 to 20 nm scale. For all samples, a logarithmic range of 40 time values (t) of 0.1–5000 ms was used. For each time, 8 repetitions were performed with a 2 s waiting time between them. The longitudinal relaxation time T_1H was obtained from Eq. (2):

$$M_z(t) = M_0 \left[1 - 2\exp\left(-\frac{t}{T_1} \right) \right] \qquad (2)$$

which can be rewritten as Eq. (3):

$$\ln\left(\frac{M_0 - M(t)}{2M_0} \right) = -\frac{t}{T_1} \qquad (3)$$

where M_0 is the maximum or equilibrium magnetization; $M(t)$ is the magnetization at each recovery time t and ($-1/T_1$) is the angular coefficient of the line. Since the longitudinal relaxation process in polymeric systems is governed preferably by spin diffusion processes in coupled domains, it is possible to trace an estimation of the nanometer path traveled by the magnetization during the spin relaxation through Eq. (4):

$$r = \sqrt{6nDt} \qquad (4)$$

where n is a factor related to domain dimensions. In this case $n = 3$. For the self-diffusion coefficient D, the polyethylene value of 0.83 $nm^2 \cdot ms^{-1}$ was used along with the longitudinal relaxation time of each sample for t.

Scanning electron microscopy (SEM)

SEM micrographs were obtained by an SEI model Quanta 200 microscope, and samples were coated with silver.

Fourier-transform infrared (FT-IR) spectroscopy

FTIR spectra were generated with a Perkin Elmer Frontier FT-IR/FIR. The technique used was ATR (attenuated total reflectance) using a diamond/ZnSe crystal, in the wave number range of 4000–400 cm^{-1} with 60 scans and 4 cm^{-1} resolution.

X-ray diffraction analysis (XRD)

A Rigaku Ultima IV X-ray diffractometer was employed to obtain diffraction patterns for samples of raw jute fiber, chemically purified fiber and fibers with the modified surface. These were measured using Cu-filtered Cu Kα radiation (λ = 1.5406 Å) at 30 kV and 15 mA, with 2θ of 2–40° and with goniometer speed of 0.5°/min. The crystallinity index (CI, %) was determined by Eq. (5):

$$CI = \left(1 - \frac{I_{am}}{I_{200}} \right) \cdot 100 \qquad (5)$$

where I_{200} is the height of the 200 peak (I_{200}, 2θ = 22.6º) and I_{am} is the minimum between the peaks at 200 and 110 (I_{am}, 2θ = 18º) [34].

Thermogravimetric analysis (TGA)

This analysis was performed with a TA Series Q Model 500 analyzer. The comparison of thermal degradation profile of the samples, from raw fibers to modified ones, was performed using a temperature range from room temperature to 973 K under inert atmosphere, at a heating rate of 10 K/min.

3. Results and Discussion

3.1. Visual Test

The fibers JF, JF_Cl, JF_al, JF_ha, JF_Ti, JF_APTMS, and JF_Ti+APTMS were suspended in water, and the JF_ha was also suspended in methanol and isobutanol using an Ultra Turrax dispersor for 2 min at 20,000 rpm. Fig. 2 shows photos of the water suspensions taken after 30 min rest. The change in color and dispersion of fibers can be an indication of the removal of substances, such as lignin and hemicellulose, after the chemical treatments applied. More stable suspension can be generally observed for purified and modified fibers compared to the JF and JF_Cl fibers. Phase separation (suspension and water) is observed for all samples, but the JF_ha fiber is better dispersed. The probable formation of a double layer of electric repulsion between the suspended microfibrils due to the sulfate groups attached to the fiber surface allows a better dispersion in water [22]. The modified fibers showed higher precipitation, observed especially for the JF_Ti fibers, followed by the JF_APTMS and JF_Ti+APTMS in that order, probably due to the increase in fiber density. Although not expected, the fibers modified with both Ti and silane treatments showed better dispersion in water than those treated separately.

Suspensions of JF_ha fibers in water, methanol and isobutanol were observed and are shown in Fig. 3. JF_ha fibers are better dispersed in water because of higher hidrophilicity. The increase in decantation is proportional to the reduction of polarity of the solvents used, as shown in Fig. 2.
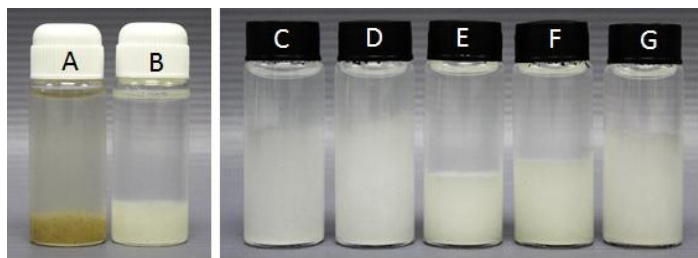
Fig. 2. Dispersion of jute fibers in water: JF (a); JF_Cl (b); JF_al (c); JF_ha (d); JF_Ti (e); JF_APTMS (f) and JF_Ti+APTMS (g)
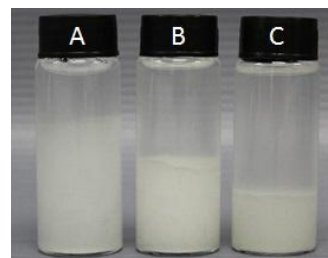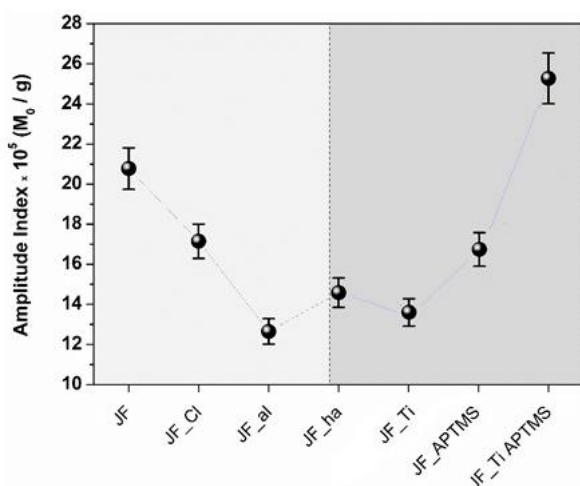

Fig. 3. Suspensions of JF_ha in water (a); methanol (b) and isobutanol (c) after 30 min rest

3.2. Low-Field NMR Measurements
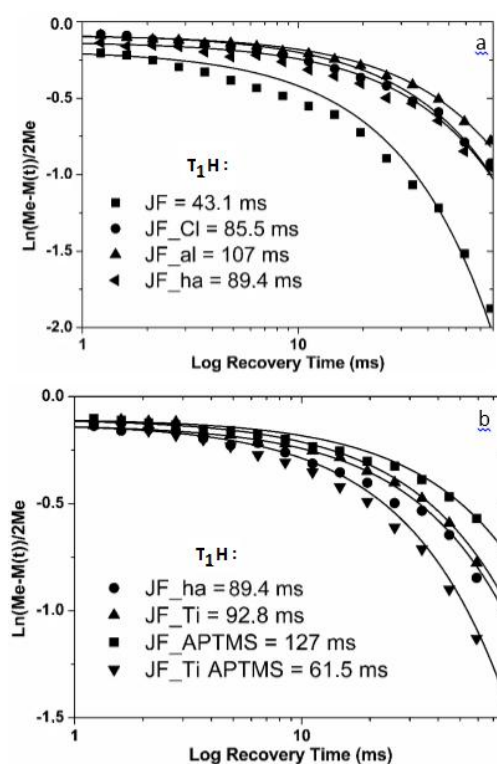
Fig. 4 shows the variation of the amplitude indices (*AI*) for the various fibers after treatment. A reduction of these values can be seen due to the removal process of the non-cellulosic materials (light gray) and a rise in the stages of superficial modification, with the addition of groups containing hydrogen. The decrease of *AI* for sample JF_al shows that the hydroxyl groups changed to alkoxide ones. The increase observed for the sample JF_ha is further indication of the presence of sulfate groups adhered to the fiber surfaces, and may influence the increase of moisture absorption of the fibers after this step. Modification of fibers with TiP shows the decrease of *AI*, which is in accordance with the idea of introducing titanium oxide in place of some hydroxyl groups on the cellulose surface. On the other hand, silanization further enhances *AI* due to hydrolysis of trimethoxy-silane. Therefore, fixation of silane increases the amount of OH groups on the cellulose surface. Again, there is a disruption of behavior in the fibers where both TiP and silane were introduced, and *AI* sharply increases.

Fig. 5a presents the graph that allowed calculating the relaxation time T_1H. An increase of T_1H can be observed as a function of the amorphous phase removal, proving the continuous decrease of the noncellulosic domains of greater mobility as a function of the extraction processes, which results in longer relaxation time of more rigid cellulose chains. Therefore, the increase in T_1H is consistent with the extraction of lignin and hemicellulose in samples JF_Cl and JF_al. The drop observed for the JF_ha sample is due to the greater string spacing obtained by the insertion of the sulfate groups after the acid hydrolysis. This decrease indicates that the 10% solution of H_2SO_4 under the reaction conditions described earlier, in addition to increasing mobility of the cellulose chains, does not attack the amorphous phase by isolating the rigid crystalline structures.

Fig. 4. Amplitude indices calculated from the initial decay signal (M_0) obtained by the solid echo sequence and divided by the mass of each sample


Fig. 5. Curves of longitudinal relaxation obtained by inversion-recovery: purified cellulose (a) and modified cellulose (b). The solid lines represent the fit for each sample according to Eq. (2)

Fig. 5b shows the variation of T_1H as a function of the chemical modification performed in the hydrolyzed fibers (JF_ha) – titanation, silanization and with both TiP and APTMS. The strong increase of T_1H for the JF_APTMS sample indicates intermolecular hydrogen bonding interactions between the cellulose hydroxyl groups and the APTMS amine group. In contrast, for the sample obtained after both TiP and silane, a sharp drop in the relaxation time is due to the presence of the modifying groups on the surfaces of the fibers, acting as spacers and plasticizers, greatly reducing the stiffness of the polymer accompanied by a decrease in the thicknesses of the crystalline domains (r). Therefore, the doubly modified fiber (JF_Ti+APTMS) shows much shorter relaxation time with greater amplitude index. It is possible that in this case polysiloxane was formed on the surface, because most of the OH species were occupied with Ti oxide. This could explain the previous observation of better dispersion of these fibers in water.
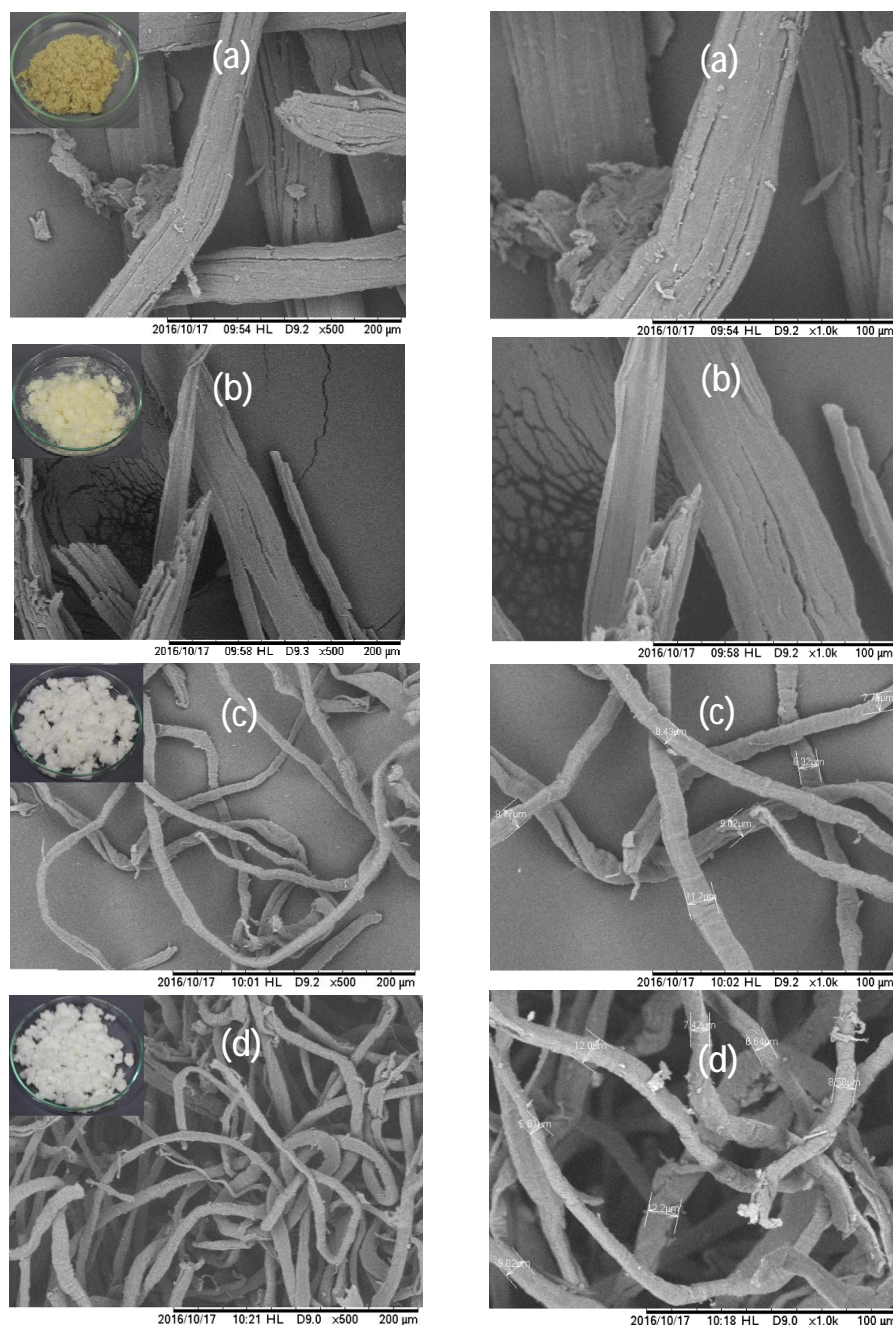
Fig. 6. SEM micrographs of samples: JF (a); JF_Cl (b); JF_al (c) and JF_ha (d) with 500x magnification (photos of the dried fibers are inserted) and 1000x
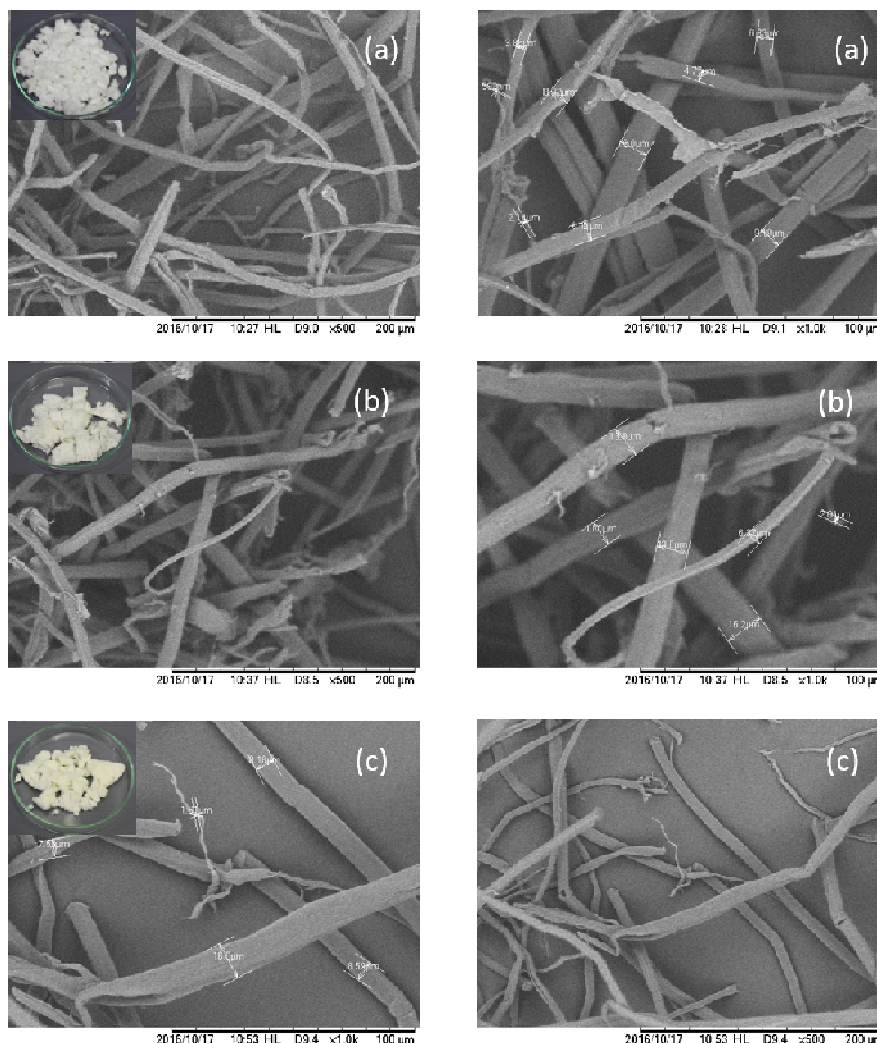
Fig. 7. SEM micrographs of the samples JF_Ti (a); JF_APTMS (b) and JF_Ti+APTMS (c) with 500x magnification (with photos inserted) and 1000x

3.3. Morphology by Scanning Electron Microscopy (SEM)

The SEM micrographs in Fig. 6 show the effect of treatments on fiber morphology due to the removal of lignin and hemicellulose and after acid hydrolysis with sulfuric acid. The observed structure for the JF fiber (Fig. 6a) is similar to the JF_Cl bleached sample (Fig. 6b), where fibers have large diameters and thinner fibers are attached to each other, as well as cracks along them. However, the surface of the JF_Cl fibers appears free of particles, and a distinct change in color can be observed in the photos accompanying the micrographs.

Only after removal of most of the hemicellulose by treatment with NaOH a significant change in the diameter of the fibers could be observed, showing fibrillation, and the diameters decrease from around 30–50 μm to 7–11 μm

(Fig. 6c). The added photos also show changes in fiber JF_al, which are whiter.

After treatment with H_2SO_4 (Fig. 6d), the length of the individual JF_ha fibers was maintained, indicating the preservation of the amorphous domains of cellulose chains, corroborating the NMR results shown in the curve of Fig. 5a. However, fibers with smaller diameters (below 2 μm) are observed due to further fibrillation. This was probably owing to a change in the interaction between the fibrils caused by the insertion of the sulfate groups.Fig. 7 presents the micrographs of samples treated with TiP, APTMS, and doubly treated. Generally, it can be observed for all treated fibers that the diameter decreased to about 1 μm, a sign of greater fibrillation. However, the micrographs shown in Fig. 7c indicate that the doubly treated fibers have even smaller diameter. It is important to mention that after Ultra Turrax dispersion, the smaller fibers did not aggregate when dried.

3.4. Infrared Spectroscopy (FTIR)

FTIR spectroscopy was performed to characterize the variations in the chemical structure of jute fibers after different treatments, through the identification of the functional groups present. All treatments promoted variations in the fibers physico-chemical properties, resulting in effective removal of the main amorphous components, lignin and hemicellulose, after subsequent chemical treatments. In addition to the visual changes observed by SEM micrographs, Fig. 8 shows the difference between the FTIR spectra for untreated JF samples and each step of the chemical treatment performed.

Dominant peaks in the 3300 cm^{-1} region relative to the stretching of the O–H bonds and at 2880 cm^{-1}, related to the C–H stretching in saturated hydrocarbons, can be observed in all spectra. After bleaching with NaClO$_2$ (spectrum (b)), the peak intensities at 1513 and 1460 cm^{-1}, representing the aromatic ring C=C vibration, decreased, as did the deformation vibration of lignin C–H. These changes are apparent in spectrum (a) in the raw jute fibers [2]. These peaks are no longer observed after treatment with NaOH, as well as the band at 1724 cm^{-1}, assigned as the acetyl ester and uronic groups of hemicellulose.

Moreover, the band at 1230 cm^{-1}, typical of C–O functional group corresponding to aryl-alkyl ether in lignin, disappeared, indicating removal of both hemicellulose and lignin, confirming the results of NMR previously described [35]. The peaks observed at 1603 and 1645 cm^{-1} can be attributed to the H–O–H stretching vibration of the absorbed water [36]. The increase in peak intensity around 1100 and 1050 cm^{-1} can be ascribed to the increase in cellulose content due to the removal of the other fiber components. Furthermore, the peak at 1100 cm^{-1} can be attributed to the symmetrical glycosidic stretching of cellulose (C–O–C), while the peaks in the region of 1060–1050 cm^{-1} are assigned to the stretching of C–OH bonds [37, 38].

Fig. 9 shows the spectra of the treated fibers compared to the hydrolyzed one. In general, the spectra shown in previous figures are very similar to those of titanized and silanized cellulose fibers. Alteration in spectrum (b) corresponding to silanized fiber was detected through the appearance of characteristic peaks that indicate the chemical bonds in APTMS. Two peaks at 1260 and 800 cm^{-1} are attributed to Si–O–C and Si–C stretching, respectively [39]. However, there was no significant change in the presence of TiO$_2$ [29] in the spectra of both JF_Ti and JF_Ti+APTMS.
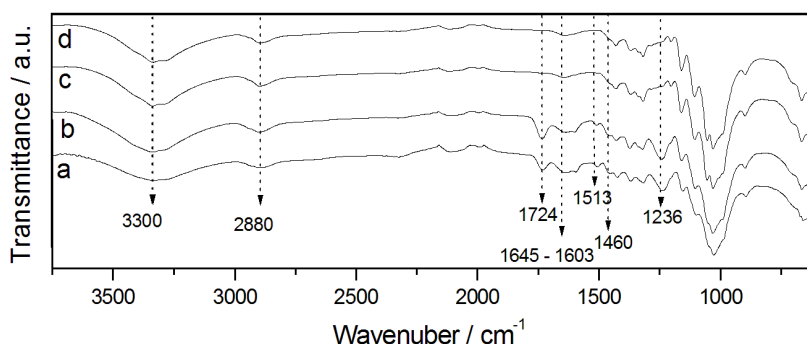
Fig. 8. FTIR spectra of the samples: JF (a); JF_Cl (b); JF_al (c) and JF_ha (d)
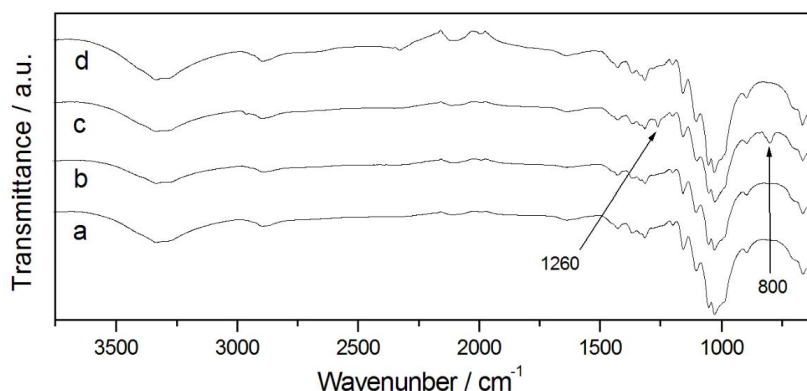
**Fig. 9.** FTIR spectra of the samples: JF_ha (a); JF_Ti (b); JF_APTMS (c) and JF_Ti+APTMS (d)

3.5. X-Ray Diffraction (XRD) Analysis

The X-ray diffraction patterns of the untreated and chemically treated jute fibers are shown in Fig. 10. The diffractograms of all samples show the presence of reflections at $2\theta = 16°$ and $22.6°$, which represents the crystalline pattern of cellulose I, indicating that the crystalline structure of the cellulose was not altered in the bleaching, alkali or hydrolysis treatments performed in this work. The removal of lignin and hemicellulose was accompanied by increased crystallinity (Table 2), which ranged from 66.5 % for raw jute to 68.1 % for JF_Cl fibers, due to the removal of most lignin, as confirmed by FTIR. After treatment with NaOH, the crystallinity of JF_al fibers increased to 74.5 % due to removal of hemicellulose and residual lignin, also evidenced by FTIR spectra. Crystallinity of 78.6 % was obtained after treatment with sulfuric acid. Although a high crystallinity index (*CI*) was observed, other results already discussed here suggest that the amorphous region of the cellulose chain was not extensively attacked, remaining intact after acid hydrolysis with low H_2SO_4 concentration. The high crystallinity of microfibrils may be more effective in obtaining reinforcements for composite materials [1, 2]. Table 2 also shows the thicknesses of crystalline domains obtained by NMR through Eq. (4), based on the respective T_1H values. A tendency higher crystallinity index is observed by increasing the thickness of the crystalline domains r up to the alkali treatment. After hydrolysis, some decrease in r was observed.

Cellulose modification with TiP or silane separaely tended to increase both *CI* and r. For the sample modified with TiP there was no significant difference in the crystallinity degree, presenting *CI* of 82.0 %. However, the reduction of r was associated with the presence of TiO_2 species, hindering the packing of the cellulose chains. No additional reflection was observed in the diffractograms associated with TiO_2, which is probably amorphous. However, the increased crystallinity of APTMS-modified fibers (82.6 %) was accompanied by increased thickness of crystalline domains r, as revealed by NMR.

Once again, the treatment with both reagents produced different results, since the trend was to decrease *CI* and r. This confirms the synergetic behavior of those treatments, decreasing both the degree of crystallinity and size of crystalline domains of cellulose fibers. As already mentioned, this could be due to the formation of polysiloxane on the fiber surface. According to the literature [33], a reduction in the *CI* value of silanized cellulose fiber is expected due to the formation of polysiloxane structures. Such large coupling molecules upset the packing of the cellulose chains to some extent. Polysiloxane was formed only after some OH groups were occupied with Ti species.
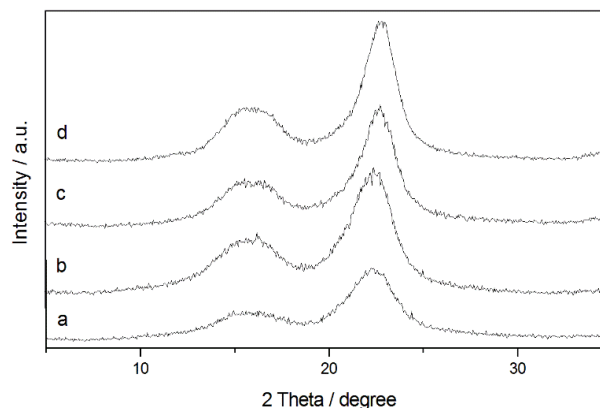
Fig. 10. X-ray diffractograms of the samples:
JF (a); JF_Cl (b); JF_al (c) and JF_ha (d)

Table 2

**Crystallinity index and crystalline domain size of raw, purified and modified jute fibers**

Sample	*CI*, %	r, nm
JF	66.5	14.6
JF_Cl	68.1	20.6
JF_al	74.6	23.1
JF_ha	78.6	21.1
JF_Ti	82.0	21.5
JF_APTMS	82.6	25.1
JF_Ti+APTMS	66.1	17.5

The X-ray diffraction patterns of the modified fibers are shown in Fig. 11. The diffractogram of the hydrolyzed sample JF_ha is added for comparison. A marked decrease in crystallinity can be noticed for the JF_Ti+APTMS sample, accompanied by reduction of r, indicated by broadening of the cellulose crystalline reflection.

3.6. Thermogravimetric Analysis (TGA)

Thermal degradation of a material can be evaluated by mass loss as a function of temperature due to the formation of volatile products through degradation. This characteristic is important to evaluate thermal degradation resistance when the polymer composite preparation process uses high temperatures. Fig. 12 shows the thermograms of raw jute fibers, the fibers obtained in all chemical purification steps and the chemically modified fibers. All samples exhibited small mass loss between 298–423 K, corresponding to the loss of absorbed moisture. It is also possible to observe that this loss of mass is smaller for the modified fibers, with JF_Ti having least loss. This fact shows the increase in hydrophobicity of the fibers treated with TiP. The values obtained from Fig. 12 are represented in Table 3. Both JF and JF_Cl fibers exhibited three events in the degradation curve. The

first, common to all samples, is attributed to the loss of absorbed water. The second, in the temperature range of 473–573 K, is attributed to pyrolysis of hemicellulose. The third event between 553 and 673 K, also common to all samples, is attributed to degraded components of higher molar mass like cellulose. In general, the chemically modified fibers presented higher resistance to thermal degradation; especially JF_Ti+APTMS, with initial degradation (temperature of 2% mass loss, $T_{0.02}$) achieving 554.4 K.
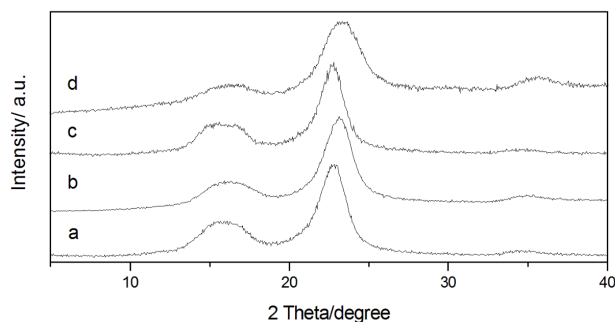
Fig. 11. X-ray diffractograms of the samples: JF_ha (a); JF_APTMS (b); JF_Ti (c); and JF_Ti+APTMS (d)
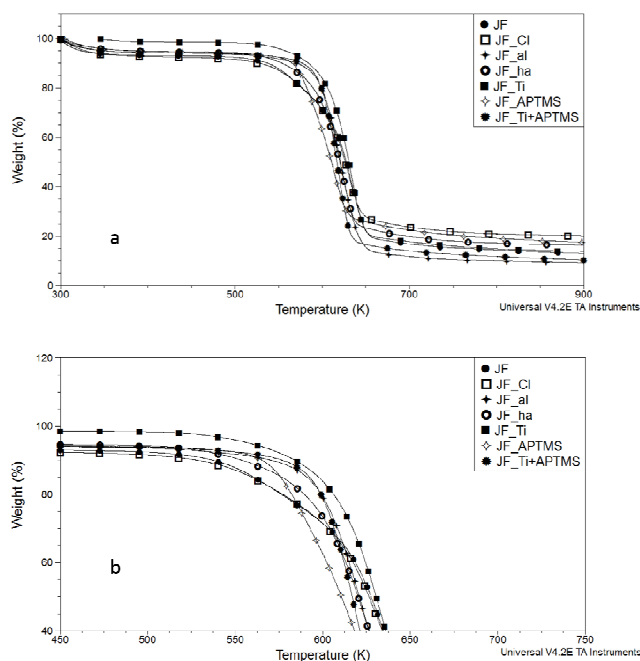
Fig. 12. TGA profiles of the samples JF, JF_Cl, JF_al, JF_ha, JF_Ti, JF_APTMS and JF_Ti+APTMS. Temperature ranges (K): 298–972 (a) and 493–653 (b)

Table 3

Thermal properties of raw, purified and modified jute fibers

Sample	Initial mass loss, %	$T_{0.02}$, K	T_{max}, K
JF	6.8	525.4	565.1/634.6
JF_Cl	7.2	519.0	573.3/630.7
JF_al	5.7	541.4	621.8
JF_ha	6.1	531.1	624.3
JF_Ti	1.2	543.1	634.2
JF_APTMS	5.1	547.8	588.0/614.8
JF_Ti+APTMS	5.7	554.4	618.6

4. Conclusions

Cellulose fibers with reduced diameter and altered structure were obtained from the chemical purification and surface modification of jute fibers. FTIR spectra of fibers revealed that hemicellulose and lignin were mostly removed due to purification treatments. In comparison with the other modified fibers, those treated with both titanium and silane (JF_Ti+APTMS) behaved differently from predicted when compared with the fibers obtained by the isolated treatments. The doubly treated fibers could be better dispersed in water and reagglomeration did not occur after drying. NMR measurements showed a sudden increase in amplitude index due to the incorporation of high amounts of OH groups from the silane, indicating the formation of polysiloxane. Moreover, a sharp drop in

relaxation time showed a large reduction of stiffness due to the groups linked to the cellulose chains. Thickness of crystalline domains also decreased and XRD revealed the reduction of the crystallinity degree to around 66%. However, TGA results revealed an increase of the initial thermal degradation $T_{0.02}$, achieving more than 554 K, confirming the very high thermal degradation resistance of this fiber.

Acknowledgments

References

[1] Chen W., Yu H., Liu Y.: Carbohyd. Polym., 2011, **86**, 453. https://doi.org/10.1016/j.carbpol.2011.04.061

[2] Chen W., Yu H., Liu Y. *et al.*: Carbohyd. Polym., 2011, **83**, 1804. https://doi.org/10.1016/j.carbpol.2010.10.040

[3] Klemm D., Heublein B., Fink H.-P., Bohn A.: Angewandte Chemie Int. Edn., 2005, **44**, 3358. https://doi.org/10.1002/anie.200460587

[4] Hult E., Larsson P., Iversen T.: Cellulose, 2000, **7**, 35. https://doi.org/10.1023/A:1009236932134

[5] Rosa M., Medeiros E., Malmonge J. *et al.*: Carbohyd. Polym., 2010, **81**, 83. https://doi.org/10.1016/j.carbpol.2010.01.059

[6] Sturcov A., Davies G., Eichhorn S.: Biomacromolecules, 2005, **6**, 1055. https://doi.org/10.1021/bm049291k

[7] Lee S., Mohan D., Kang I. *et al.*: Fibres Polym., 2009, **10**, 77. https://doi.org/10.1007/s12221-009-0077-x

[8] Nishino T., Takano K., Nakamae K.: J. Polym. Sci. B, 1995, **33**, 1647. https://doi.org/10.1002/polb.1995.090331110

[9] Satyamurthy P., Jain P., Balasubramanya R., Vigneshwaran N.: Carbohyd. Polym., 2011, **83**, 122. https://doi.org/10.1016/j.arbpol.2010.07.029

[10] Paakko M., Ankerfors M., Kosonen H. *et al.*: Biomacro-olecules, 2007, **8**, 1934. https://doi.org/10.1021/bm061215p

[11] Zhang Y., Nypelo T., Salas C. *et al.*: J. Renew. Mater., 2013, **1**, 195. https://doi.org/10.7569/JRM.2013.634115

[12] Chakraborty A., Sain M., Kortschot M.: Holzforschung, 2005, **59**, 102. https://doi.org/10.1515/hf.2005.016

[13] Sakurada I., Nukushina Y., Ito T.: J. Polym. Sci., 1962, **57**, 651. https://doi.org/10.1002/pol.1962.1205716551

[14] Aulin C., Ahola S., Josefsson P. *et al.*: Langmuir, 2009, **25**, 7675. https://doi.org/10.1021/la900323n

[15] Brinchi L., Cotana F., Fortunati E., Kenny J.: Carbohyd. Polym., 2013, **94**, 154. https://doi.org/10.1016/j.carbpol. 013.01.033

[16] Klemm D., Kramer F., Moritz S. *et al.*: Angewandte Chemie Int. Edn., 2011, **50**, 5438. https://doi.org/10.1002/anie.201001273

[17] Cherian B., Pothan L., Nguyen-Chung T. *et al.*: J. Agricult. Food Chem., 2008, **56**, 5617. https://doi.org/10.1021/jf8003674

[18] Cherian B., Leao A., Souza S. *et al.*: Carbohyd. Polym., 2010, **81**, 720. https://doi.org/10.1016/j.carbpol.2010.03.046

[19] Khalil H., Davoudpour Y., Islam M. *et al.*: Carbohyd. Polym., 2014, **99**, 649. https://doi.org/10.1016/j.carbpol.2013.08.069

[20] Eyholzer C., Bordeanu N., Lopez-Suevos F. *et al.*: Cellulose, 2010, **17**, 19. https://doi.org/10.1007/s10570-009-9372-3

[21] Heux L., Chauve G., Bonini C.: Langmuir, 2000, **16**, 8210. https://doi.org/10.1021/la9913957

[22] Orts W., Shey J., Imam S. *et al.*: J. Polym. Environ., 2005, **13**, 301. https://doi.org/10.1007/s10924-005-5514-3

[23] O'Regan B., Moser J., Anderson M., Graetzel M.: J. Phys. Chem., 1990, **92**, 8720. https://doi.org/10.1021/j100387a017

[24] Sunada K., Kikuchi Y., Hashimoto K., Fujishima A.: Environ. Sci. Technol., 1998, **32**, 726. https://doi.org/10.1021/es970860o

[25] Christensen P., Curtis T., Egerton T. *et al.*: Appl. Catal. B-Environ., 2003, **41**, 371. https://doi.org/10.1016/S0926-3373(02)00172-8

[26] Suty S., Petrilakova K., Katuscak S. *et al.*: Cellulose Chem. Technol., 2012, **46**, 631.

[27] Marques P., Trindade T., Neto C.: Compos. Sci. Technol., 2006, **66**, 1030. https://doi.org/10.1016/j.compscitech.2005.07.029

[28] Kelley S., Filley J., Greenberg A. *et al.*: Int. J. Polym. Anal. Character., 2012, **7**, 162.

[29] Uddin M., Cesano F., Bonino F. *et al.*: J. Photochem. Photobiol. A, 2007, **189**, 286. https://doi.org/10.1016/j.jphotochem.2007.02.015

[30] Daoud W., Xin J., Zhang Y.: Surf. Sci., 2005, **599**, 69. https://doi.org/10.1016/j.susc.2005.09.038

[31] Kalia S., Kaith B., Kaur I.: Polym. Eng. Sci., 2009, **49**, 1253. https://doi.org/10.1002/pen.21328

[32] Mahshid S., Askaria M., Ghamsarib M. *et al.*: J. Alloy Compd., 2009, **478**, 586. https://doi.org/10.1016/j.jallcom.2008.11.094

[33] Rong M., Zhang M., Liu Y. *et al.*: Compos. Sci. Technol., 2004, **61**, 1437. https://doi.org/10.1016/S0266-3538(01)00046-X

[34] Moran J., Alvarez V., Cyras V., Vazquez A.: Cellulose, 2008, **15**, 149. https://doi.org/10.1007/s10570-007-9145-9

[35] Rahman M., Afrin S., Haque P.: Progr. Biomater., 2014, **3**, 1. https://doi.org/10.1007/s40204-014-0023-x

[36] Fatah I., Khalil H., Md Hossain S. *et al.*: Polymers, 2014, **6**, 2611. https://doi.org/10.3390/polym6102611

[37] Gwon J., Lee S., Chun S. *et al.*: Korean J. Chem. Eng., 2010, **27**, 651. https://doi.org/10.1007/s11814-010-0058-1

[38] Vazquez N., Garcia T.: J. Mexican Chem. Soc., 2010, **54**, 192.

[39] Kim D., Dhand V., Rhee K., Park S.: Polymers, 2015, **7**, 527. https://doi.org/10.3390/polym7030527

ХІМІЧНЕ ОБРОБЛЕННЯ ТА МОДИФІКАЦІЯ ПОВЕРХНІ ДЖУТОВОГО ВОЛОКНА

Анотація. Проведені дослідження з джутовим волокном. Для одержання волокна зі зменшеним діаметром і меншою агломерацією та адгезією до полярних полімерів, таких як поліаміди, проведені хімічні процеси очищення, механічної дисперсії в Ultra Turrax та модифікування ізопропоксидом титану (ІПТ), 3-амінопропілтриметоксисиланом (АПТМС), а також подвійне модифікування ІПТ і АПТМС. За результатами СЕМ встановлено, що після висушування та подрібнення в порошок волокна мають діаметр близько 10 мкм. Встановлено, що волокна, оброблені лугом, гідролізовані кислотою і двічі модифіковані, добре диспергують у воді. СЕМ мікрофотографії свідчать, що волокна, модифіковані ІПТ і АПТМС, мають діаметр близько 1 мкм. Результати ЯМР аналізу доводять зниження індексу амплітуди, що супроводжується збільшенням часу релаксації і товщини кристалічних доменів внаслідок видалення лігніну і геміцелюлози. Протилежний ефект спостерігався у випадку хімічного модифікування. Результати ІЧ-Фур'є спектроскопії та рентгенівської дифракції також доводять видалення лігніну і геміцелюлози. Показано, що індекс кристалічності (ІК) в джутовому волокні збільшується при видаленні аморфних компонентів, і зменшується у волокнах, модифікованих ІПТ і АПТМС. Результати ТГА вказують на вищу стійкість до термічного розкладання при подвійному модифікуванні волокна.

Ключові слова: джутове волокно, целюлоза, оксид титану, силанізація.